Experimental thermodynamic first and second law analysis of a variable output 1-4.5 kWe, ICE-driven, natural-gas fueled micro-CHP generator

Zachary Taie*, Christopher Hagen

Oregon State University, School of Mechanical, Industrial, and Manufacturing Engineering, 1500 SW Chandler Ave., Bend, OR 97701, U.S.

Abstract

This work experimentally assesses the thermodynamic performance of the only single kWe, variable-output, continuous duty, internal combustion engine driven, residential micro-combined heat and power (mCHP) generator (Marathon Engine Systems ecopower) available in the United States. The system underwent steady state testing over its full operating range, and first (energy) and second (exergy) law analyses were conducted on the collected data. At rated speed, first law results reveal the ecopower operated at an electrical efficiency of 24.4±0.7% and a utilization factor of 94.5±12.6%. At the same speed, the ecopower's second law electrical efficiency was 24.3±0.8% and total second law efficiency (including exergy in both the recovered heat and electrical streams) was 33.7±1.9%. This total second law efficiency was higher than that of common residential heating devices, including electric and gas furnaces and boilers, electric air-source heat pumps, and gas-engine driven heat pumps. Further, the ecopower outperformed most of these devices at all part-load conditions as well, indicating it would be an appropriate choice for a dispatchable generator to provide ancillary grid-support services in a future with increased variable renewable generator penetration. System-level and internal combustion engine irreversibilities are also presented to identify areas of inefficiency. The most prominent irreversibilities were (in decreasing magnitude) irreversible heat transfer, combustion irreversibility, frictional and pumping losses, followed by generator and power electronic losses.

Keywords: Residential cogeneration, variable output micro-combined heat and power, thermodynamic exergy analysis, natural gas, internal combustion engine, dipatachable grid balancing CHP

* Corresponding author. Tel.:+1-541-579-5673.
E-mail address: taiez@oregonstate.edu.

1. Introduction

1.1. Motivation

The combined efficiency of the United States's electrical generation and distribution system (delivered electricity compared to primary energy consumption) was 33.6 % in 2016. This includes losses incurred in the generator during conversion from primary fuel to electricity, as well as electrical transmission and distribution losses. There are two primary routes to increase this efficiency: improve the average centralized prime mover and generator efficiency, or decrease the transmission and distribution losses. Investigating these options in closer detail reveals that state-of-the-art centralized generators have seen a steady improvement in efficiency at a rate of approximately 0.5% annually since the 1960's [1], with flagship 1.2 GW combined cycle plants currently achieving an efficiency of 63%[†] [2]. As this new technology diffuses into the generation fleet the average generation efficiency will increase as well. However, the electrical grid has not matched this level of technical improvement, with transmission and distribution losses remaining relatively flat over the last decade in the U.S. and over several decades globally [3]. This trend is mostly due to the large cost associated with rewiring transmission lines with more efficient and robust conductors that have lower resistivity or the ability to operate at a higher voltages.

Nomenclature

ARPA-E	Advanced Research Project Agency – Energy
CHP	Combined Heat and Power
mCHP	micro-CHP
DG	Distributed Generation
DOE	Department of Energy
GIMEP	Gross indicated mean effective pressure
HC	Hydrocarbon
HHV	Higher Heating Value
ICE	Internal Combustion Engine
LHV	Lower Heating Value
NIMEP	Net indicated mean effective pressure
PIMEP	Pumping indicated mean effective pressure
RMS	Root Mean Square

An approach to reduce transmission losses that does not require rewiring transmission and distribution lines is distributed generation (DG). This technique, which has seen an increase in interest recently, moves away from the traditional centralized generator model to one in which a large number of smaller generators are located closer to the site of electricity consumption. This spatial relocation

[†] All efficiencies presented will be based on the fuel's lower heating value (LHV).

of the electrical generation eliminates the need for electrical transmission and distribution, removing the associated losses. In the United States, these losses averaged 6% of the total electricity generation over the last decade. In 2016 alone these losses totaled 314 PWh, which had an associated retail value of $32 billion [4]. The power generation sector could eliminate a substantial portion of these losses if distributed generation was to see widespread adoption. Further, the use of a coordinated fleet of distributed dispatchable generators could be used to provide ancillary grid services, such as demand response or supplemental generation, to support variable renewable generators. As renewable generator penetration continues to increase these services are expected to become increasingly necessary to maintain grid stability.

There are two major barriers to overcome before widespread distributed generator adoption occurs – increasing generator efficiency (reducing O&M cost) and reducing capital cost. Currently, natural gas fueled, internal combustion engine (ICE) driven, residential backup generators (~7 kWe) have a peak electrical efficiency of approximately 21.5% [5] (LHV based). Therefore, small generators cannot currently thermodynamically outperform the centralized-generation model, and would in fact reduce the overall electrical system efficiency if implemented. To overcome this limitation, generator manufacturers have designed a new class of cogeneration units in which the generator's waste heat is utilized to satisfy residential thermal loads. This technique is termed combined heat and power (CHP), or micro-CHP (mCHP) when utilized at the residential scale (below ~50 kWe). There are several commercial systems available with an electrical output under 5 kWe, the best of which have electrical efficiencies of approximately 28.6% [6] (LHV based). These systems have total utilization factors (useful heat output plus electrical output over total heat input) approaching 100% (LHV based), and as such would increase delivered energy efficiency vs the combined natural gas and electrical grid. Internal combustion engines also provide the ramping capabilities necessary to provide ancillary grid services. These systems are therefore seeing an increase in popularity, but have low consumer penetration due to their high capital cost and long payback periods.

In an attempt to spur innovation in mCHP technology, the Department of Energy's (DOE) Advanced Research Project Agency – Energy (ARPA-E) created a program (GENSETS [7]) to fund the development of more efficient and lower cost mCHP technology. This program specifically targeted heat engine based technology, as fuel cell mCHP units have been investigated in other programs and were further from the cost targets than more mature ICE based units. The work presented here is part of a program that was undertaken to establish the current performance benchmark of state-of-the-art of mCHP generators of various sizes. The findings were provided to the ARPA-E to assist with development of the GENSETS program objectives [8].

There has been a substantial amount of work conducted recently with regard to mCHP. Much of the published work has consisted of computational studies of the potential economic [9]–[25] and

environmental impacts [11]–[14], [19], [20], [25]–[29] of implementing mCHP. However, there are several shortcomings in the current literature that need to be addressed in order to further mCHP technology: 1) most of the computational studies identified in the literature rely on performance metrics provided by manufacturers ([10], [13], [14], [21]–[25], [27], [30], [31]) which may not be impartial, and 2) the experimental performance metrics reported are largely system level (e.g., system electrical efficiency, system utilization factor, etc.) and do not provide detailed component level information (e.g., ICE thermal efficiency, mean effective pressure, generator conversion efficiency, etc.) that are necessary for technology development.

This work aims to address each of these shortcomings by: 1) providing updated system-level heat recovery and electrical efficiency as a function of engine speed for use in updating and developing dispatchable mCHP models, and 2) presenting a detailed energy and exergy accounting of each energy conversion step from the fuel's chemical energy to the output electricity, including internal combustion engine and generator performance.

2. Materials and Methods

2.1. Generator Selection

The work reported in this paper was part of a larger effort to benchmark the most technically advanced and commercially relevant generators in the nominally 1 kWe [32], 5 kWe (this study), and the 7 kWe [5] output ranges. To this end, a generator model was selected in each of these size ranges and underwent performance testing.

The first step in the generator selection process was to identify all nominally 5 kWe generators that were commercially available. This was accomplished through two processes. The first was to purchase a database from Power Systems Research that contained every model of natural gas-fueled, internal combustion engine driven, residential generators between 0-100 kWe in which more than 50 units were use in the U.S. in 2014 [33]. After reviewing the Power Systems Research database, it was clear that there was a lack of nominally 5 kWe mCHP units in service in the U.S. in 2014. In fact, the database included only a single model, indicating that only one system had more than 50 units in service nationally in 2014. However, previous investigation indicated that there was more than one commercially available mCHP generator in the 5 kWe range that was not present in the database, implying these models had a negligible market penetration in the U.S.

To identify commercial mCHP technology in the 5 kWe range that was either in use outside of the U.S., or suffering from negligible deployment domestically, an international technology survey was conducted. This survey revealed 26 commercial mCHP units with outputs between 1-10 kWe, 11 of which were in the nominally 5 kWe output range. This list was then reduced to three units based on utilization factor (electrical plus thermal efficiency) and the feasibility of importing a unit into the

U.S. for testing. The three remaining units were the SenerTec Dachs family (the standard, condensing, and low NO_x variants), the Yanmar CP5WN, and the Marathon Engine Systems ecopower. Their representative manufacturer provided specifications are compared in Table 1.

Table 1. Relevant manufacturer supplied specifications of final 5 kWe mCHP models. The Marathon Engine System was tested for this work.

Manufacturer	SenerTec				Yanmar	Marathon Engine Systems
Model	Dachs 5.5		Dachs 5.0 (Low NOx)		CP5WN	ecopower
	Standard	Condensing	Standard	Condensing		
Fuel	Natural Gas	Natural Gas	Natural Gas	Natural Gas	Natural Gas	Natural Gas
Electrical Output [kW]	5.5		5		5	1-4.5
Thermal Output [kW]	12.5	14.8	12.3	14.6	10	3.8-13.8
Fuel input [kW]	20.5		19.6		17.8	6.2-19
Electrical Input [kW]	0.12		0.12		0.33	0
Voltage/Frequency	3ø 230 V/400V 50 Hz				240 /120 60 Hz	240/60 Hz
Efficiency						
-Electrical	27%		26%		28%	25%
-Heat Recovery	61%	72%	63%	74%	56%	68%
-Utilization Factor	88%	99%	89%	100%	84%	93%
Emissions	Meets German TA-Luft				Meets EPA	Meets EPA
-CO2	< 0.3 g/Nm^3				< 610 g/kWh	327 kg/MWh
-SO2						Trace kg/MWh
-NOx	< 0.5 g/Nm^3				< 5.36 g/kWh	0.03 kg/MWh
Endurance [hr]	80,000				60,000	40,000

Upon further investigation, the factors deemed most important when choosing the 5 kWe mCHP unit were the unit's efficiency, expected lifetime (endurance), capital cost, and availability. Due to the claimed high efficiency of the Dachs units, they were left as contenders in the final selection. However, importation restrictions proved to be too cumbersome, and they were eliminated. This left only the Yanmar CP5WN and the Marathon Engine Systems ecopower. After receiving quotes from both companies (confidential), there was not a significant difference in price. The differentiating characteristic between the two units ended up being the utilization factor, where the ecopower had a 9% higher total claimed efficiency. As a secondary benefit, the ecopower, (the engine of which was originally designed by Briggs and Stratton for the York Triathlon engine-driven heat pump), was able to modulate its thermal and electrical output. This modulating capability was uncommon for the identified mCHP units in all size classes, and was an interesting contrast to the common mCHP system which has a single operating point, including the selected 1 kWe and 7 kWe models tested in this program.

2.2. Experimental Testing Range

It is typical for mCHP units to only operate at a single load point, i.e., operate in a binary on/off fashion with a single electrical output when in operation. This is common because optimizing a single load point results in a higher efficiency relative to optimizing a range of loads as design trade-offs are not as restrictive. However, binary operation results in a device that loses valuable features such as load following, or the ability to participate in market operations such as demand response or grid stabilization. As mentioned previously, the ecopower is capable of modulating its electrical output from ~1 – 4.5 kWe with an associated heat output of ~4.0 – 12.4 kW. Less than 10% of the identified mCHP generators in the 0 – 10 kWe range had the ability to modulate output, making it an uncommon attribute. This capability could theoretically allow the ecopower to respond to grid requests while still meeting the residence's electrical and thermal needs. To evaluate this capability, the ecopower was tested at the following five speeds: 1200, 1500, 1900, 2700, and 3600 RPM.

2.3. ecopower Experimental Facility

Testing of the ecopower occurred at Intertek Carnot Emissions Services with the assistance of the authors and a representative from Marathon Engine Systems. Triplicate performance and emissions data was recorded for repeatability. An instrumentation diagram detailing the location of the installed transducers is shown in Figure 1.

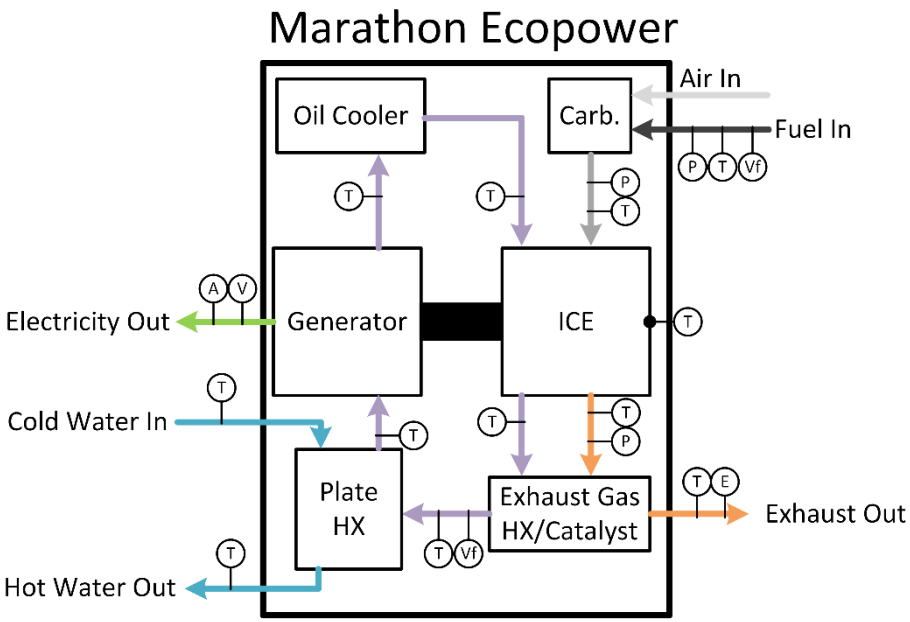

Figure 1. Instrumentation diagram of marathon ecopower. P-pressure, T-temperature, Vf-volumetric flowrate, A-amperage, V-voltage, E-emissions.

The volumetric fuel flow rate into the system was recorded using an EKM PGM-75 bellows type flow meter (±1.5%) with measurements for pressure and temperature taken using an omega px309-015CG5V pressure transducer (±1.0%) and a K type thermocouple (±1.1 °C), respectively. A carbon balance calculation using the emissions measurements was also used to verify the measured fuel flow rate, which showed agreement within ±3% for all test runs. The output voltage and current was measured with a Mastech MS2203 (±1.2%) and an Extech 380943 (±1.0%), respectively. All other temperature measurements, including the coolant loop, surface temperatures, exhaust temperatures, and water temperatures were made with type K thermocouples (±1.1 °C). The coolant volumetric flow rate was measured using an Omega FTB8010HW-PT flow meter (±1.5%), while the volumetric flow rate of the water was measured using an EKM HOT-SPWM-075 flow meter (±2.0%). The emissions measurements were made using a Rosemount NGA 2000 (±2.0%) with incorporated HFID for HC measurements, a NDIR MLT module for CO and CO2 measurements, and a chemiluminescence detector for wet NOx measurement. In order to calculate the gross indicated mean effective pressure (GIMEP), net indicated mean effective pressure (NIMEP), and pumping indicated mean effective pressure (PIMEP), in-cylinder pressure measurements were taken with a Kistler 6118BFD16A41 (±0.7% including transducer, data acquisition devices and charge amplifier) at >0.2 crank angle degree resolution measured by a BEI XHS25 shaft encoder (±0.1%).

Prior to data collection, the ecopower was run at rated power output until the exhaust and inlet water temperature did not change more than 0.5 °C for 10 minutes, indicating that steady state was reached. The ecopower's outlet water temperature was held at 70 °C for all testing runs, and the inlet water temperature was allowed to adjust to reach steady state. After data was collected for approximately 10 minutes at 3600 RPM the speed was reduced to 2700 RPM and the exhaust and inlet water temperatures were allowed to reach steady state. This process was repeated until data was collected at each load point (each engine speed).

2.4. Electric Motor Testing

The measured electrical production and fuel consumption of the Ecopower was sufficient to calculate the system level electrical efficiency, but a more in-depth analysis of the internal subsystems, including the engine and generator, was desired. The ecopower's control system had safeties and interlocks in place that would prevent the engine from running while disconnected from the generator, which precluded direct engine performance measurement through dynamometer testing. Therefore, to indirectly measure the engine performance, the generator's efficiency was measured through direct dynamometer testing. To calculate the engine's output shaft power the ecopower's output electrical power was modified by the generator (and assumed power electronics)

efficiency.

To couple the generator to the dynamometer a footing mount was fabricated to convert the stock engine block into a test stand. This was desirable for two reasons: 1) the generator housing was already fastened to the engine block in the stock orientation, and 2) the generator's rotor was already coupled to the crankshaft which extended through the engine block making for an easy location to couple to the torque transducer. A photograph of this arrangement is shown in Figure 2. To reduce the frictional losses as much as possible the piston was decoupled from the crankshaft and removed from the cylinder. However, the main crankshaft bearings were still located between the torque transducer and the electric generator, so the measured generator performance does include the main bearing losses, which would not normally be included in the generator efficiency. The generator's high frequency three-phase electrical output was connected to three NH Research 4600 AC electronic load banks (±0.5%), and the input shaft torque and rotational speed were measured using a Himmelstein MCRT49002V (±2 %) torque transducer.

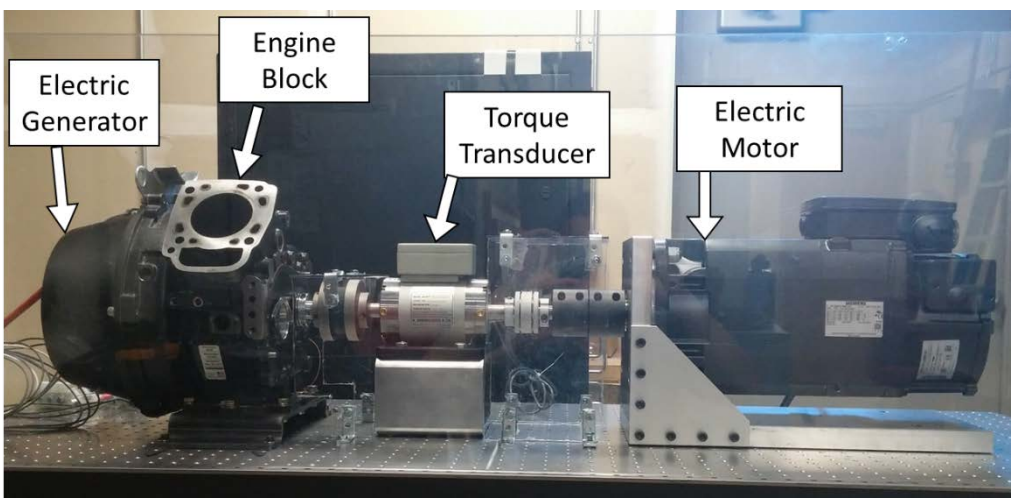

Figure 2. Electric generator testing arrangement.

2.5. Control Volume Definition, Thermodynamic Analysis, and Uncertainty Quantification

The thermodynamic analysis methodology, including control volume definition, first and second law definitions, and the uncertainty quantification has been presented in a previous sister publication [32]. For brevity, the methodology will be briefly reviewed but not rigorously defined. This description should be sufficient for those who are familiar with these analyses. For those who are not, the complete mathematical definition can be found in Taie et al. [32].

Several energy flows into and out of the ecopower were identified (most of which are shown in Figure 1), including the heat input with the fuel, thermal and chemical energy exhausted with the

exhaust gases, heat recovered in the coolant, electricity produced, and heat transfer to the environment. These energy flows were instrumented as shown in Figure 1 and were recorded as power flows at steady state. The power input via fuel was calculated by measuring the fuel input mass flow rate and the lower heating value of the fuel. The rate of recovered heat was calculated from the coolant mass flow rate, the specific heat of the coolant, and the temperature difference of the coolant leaving and entering the ecopower. The electrical power produced was calculated from root mean square (RMS) voltage and current measurements. The rate of heat leaving in the exhaust was calculated from speciated exhaust concentration measurements, the mass flow rate of the exhaust, the specific heat of the exhaust species, and the difference between the exhaust temperature and 25 °C. The rate of chemical energy leaving in the exhaust was calculated from the speciated exhaust concentration measurements, the mass flow of the exhaust, and the lower heating value of each species. The unmeasured rate of heat transfer was calculated from a first law balance around the ecopower. The utilization factor of a system is equal to the recovered heat plus work produced divided by the input energy. It is a figure of merit (similar to an efficiency) that measures a device's CHP performance.

From the second law perspective several exergy flows and irreversibilities were identified. The mass flow streams into and out of the control volume carried exergy in two forms: chemical and thermomechanical exergy. The thermomechanical exergy (calculated using the flow exergy relation) is the work that could be produced when a system is brought to thermal and mechanical equilibrium with the dead state, without an accompanying change in chemical composition. The end state of this process is termed the restricted dead state since the chemical composition of the system is not composed of species that are present in the true dead state. The chemical exergy, then, is the work that could be produced as the system undergoes chemical reactions that change its chemical composition from the restricted dead state to the true dead state. This is similar to the heating value of a fuel which is a first law view of the same process. However, there is an entropy penalty that must paid during this process, limiting the amount of work that can be produced from the chemical reaction. The chemical exergy of the fuel and exhaust streams was calculated from the Gibbs free energy of each species. Exergy was also transferred out of the system with heat transfer. The exergetic value of heat is the work that could be produced from the heat if it were supplied to Carnot heat engine at a given supply and ambient temperature. The combustion irreversibility was calculated from an entropy balance on the internal combustion engine, and the frictional and pumping irreversibilities were calculated from the in-cylinder pressure measurements.

The uncertainties presented in this paper are a combination of the known systematic errors and the measured random errors. The elemental systematic errors of each measurement device (presented in parenthesis next to each measurement device in Section 2) were combined using the root of sum of squares method to calculate the total expected systematic error of each measurement. The random error of each measurement was calculated from the standard deviation of the set of

measurements and a “t estimator” from statistical methods. The total uncertainty of each measurement is then the root of sum of squares of the random and systematic uncertainty of each measurement. The Kline and McClintock method was used to calculate the propagation of these uncertainties from individual measurements to calculated values. For a more detailed explanation of the uncertainty quantification method used see Taie et al. [32] section 2.4.4.

3. Results and Discussion

The results presented here first detail the system level performance for comparison to the state of the art and for use in updating mCHP models. Following this discussion, a detailed analysis of the energy conversion steps in the internal combustion engine and the electric generator will be presented.

3.1. System Level Results

At the system level, the primary objective was to measure the ecopower’s electrical efficiency and utilization factor as a function of engine speed. At rated speed, these measurements provide a valuable update to models that treat the mCHP generator as a binary device, while the part-load measurements provide updated (and more granular) information for dynamic mCHP models. To calculate these figures of merit, instrumentation was installed on the four main system level energy flows into and out of the mCHP system: fuel input, heat recovered in the coolant recovery loop, electrical energy, and thermal and chemical energy in the system exhaust (Figure 1). To identify the proportion of input energy (or exergy) that left the system as unmeasurable heat transfer, an energy (or exergy) balance was conducted. The energy balance is presented in Figure 3 and Figure 4, and the exergy balance is presented in Figure 5 and Figure 6.

3.1.1. First Law Results

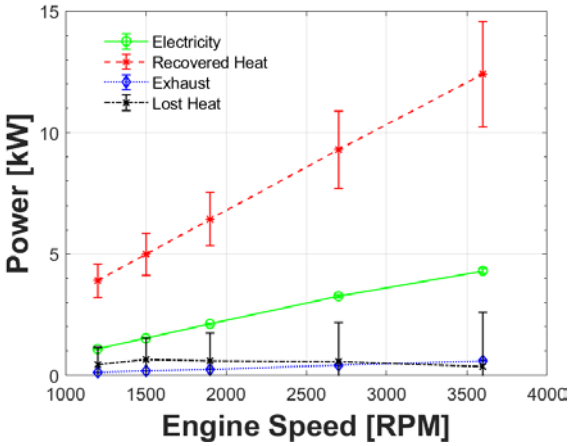

Figure 3. Output power streams of the ecopower under varying engine speeds.

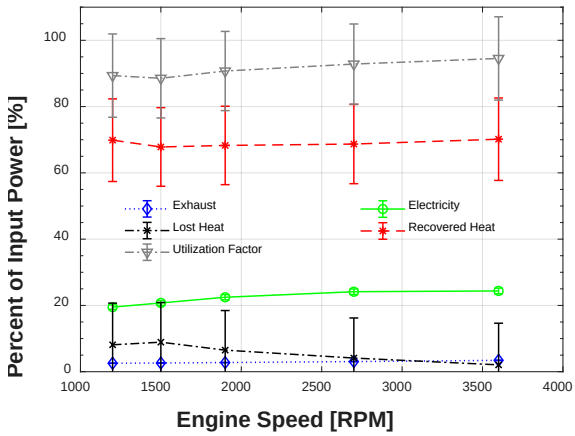

Figure 4. Percent of input power of each output power stream, defined as $\frac{\dot{E}_{stream}}{Q_{LHV}}$, along with utilization factor.

The ecopower was most efficient at higher engine operating speeds, Figure 4. A peak electrical efficiency and utilization factor of 24.4±0.7 and 94.5±12.6 %, respectively, were recorded at an engine speed of 3600 RPM. At the lowest engine speed of 1200 RPM there was a noticeable uptick in the fuel energy fraction recovered as heat, which also increased the utilization factor even as the electrical efficiency continued to decrease. This provides an interesting data point, as many HVAC control strategies can utilize consistent, low heat flows to maintain room temperatures. As a percentage of input power, the energy remaining in the stack exhaust increased slightly with engine speed, but it was largely negligible.

The magnitude of recovered heat and electricity generated were nearly linear functions of engine speed over the ecopower's operating range, Figure 3. However, the energy remaining in the engine exhaust (chemical plus thermal) showed a positive power fit to the engine speed, indicating that in-cylinder heat transfer and combustion efficiency were increasingly effected by decreased cylinder and catalyst residence times. Consequently, the energy lost to the surroundings through heat transfer decreased in response to the higher amounts of energy remaining in the exhaust at higher engine loads.

The uncertainties of the utilization and the recovered heat were primarily derived from the use of type K thermocouples which have a larger error than their type T counterparts. No type T thermocouples were available at ICES. The utilization uncertainty reaches above 100 % because the efficiency values provided are defined based on the LHV. The ecopower is actually a partially condensing unit, which means that the HHV is the maximum bounding case. The HHV limit is

approximately 110% of the LHV.

3.1.2. Second Law Results

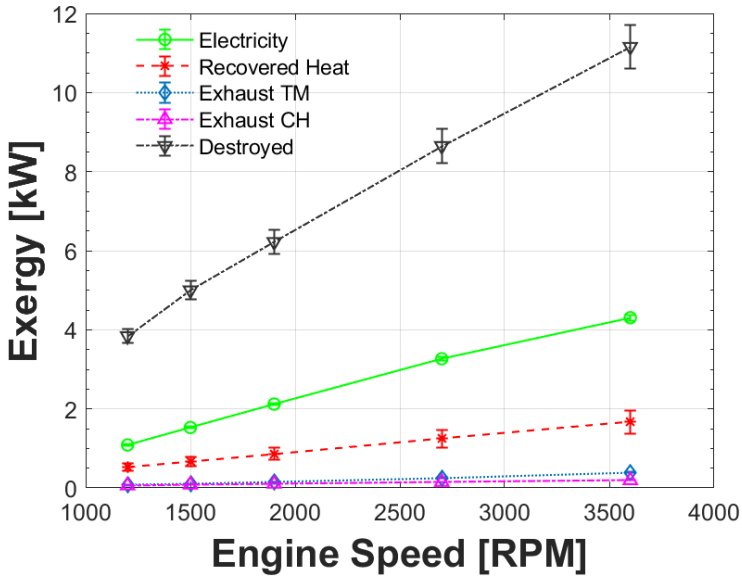

Figure 5. System-level ecopower output exergy flows. Exhaust TM – thermomechanical exergy present in the exhaust, Exhaust CH – chemical exergy present in the exhaust.

Figure 5 shows the system-level ecopower exergy outflows, including the system exergy destruction, as a function of engine speed. The major difference between the system-level exergy (Figure 5) and energy (Figure 3) outflows is the value of the recovered heat. As shown in Figure 3, the recovered heat contains approximately three times the energy present in the electricity, however, it only contains approximately half as much exergy as the electricity does. This discrepancy indicates the low quality of the recovered heat (which is recovered at approximately 70 °C). With the exception of the thermomechanical exergy present in the exhaust which shows a positive power correlation to engine speed, the exergy flows are relatively linear or flat with engine speed. At 1200 RPM the thermomechanical exergy present in the exhaust is roughly 25% higher than the chemical exergy present in the exhaust, however, this discrepancy increases to approximately 100% at 3600 RPM. This indicates that the reduced residence time has a larger impact on heat transfer within the engine cylinder and exhaust catalyst than it does on system-level chemical conversion efficiency.

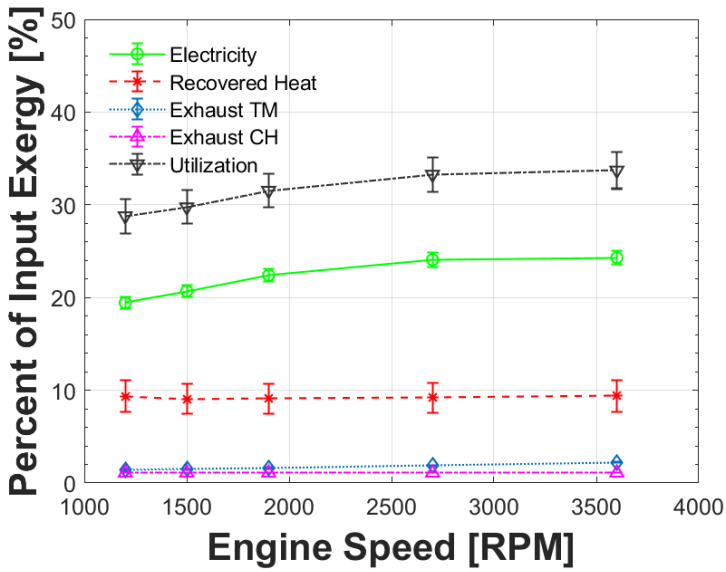

Figure 6. Exergy output streams normalized by input exergy. Exhaust TM – thermomechanical exergy present in the exhaust, Exhaust CH – chemical exergy present in the exhaust.

When the output exergy streams are normalized by the input exergy stream, the efficiency trends become clearer. The second law efficiency of the electrical stream reaches 24.3±0.8% at 3600 RPM, while the coolant stream delivers 9.4±1.7% of the input exergy at the same speed. Combined, these yield a second law utilization factor (also known as effectiveness or total second law efficiency) of 33.7±1.9%.

The ecopower's total second law efficiency is quite impressive when realizing that it is primarily a furnace. Current heating technology has been developed with an emphasis on first law heat delivery efficiency, which has resulted in maximizing the heat delivered by the device. However, this approach has yielded devices with relatively low second law efficiencies as can be seen in Table 2.

Table 2. Typical energy and exergy efficiency values for standard residential heating equipment. 1-[34], 2-[35], 3-[36], 4-[37], 5-[38].

Device	Energy Efficiency [%]	Exergy Efficiency [%]
Electric resistance heater[1]	99	6
Electric Boiler[2]	67	5
Electric Furnace[2]	54	18
Electric heat pump[1]	380	19
Gas furnace[3]	85+	10
Gas boiler[1,2,4]	90+	<10
Gas-ICE air-source heat pump[5]	176	29
Geothermal[4]	95	16
ecopower mCHP	95	34

These efficiency measurements highlight the ecopower's main thermodynamic benefit of providing electricity as well as heat. Not only does the ecopower compare favorably at rated speed, but it outperforms most of the highlighted heating appliances at all part load conditions as well. Efficiently operating at part load is important because it could allow the ecopower to efficiently deliver heat while operating in a mode in which it could either increase or decrease its electrical output. This wait-and-respond capability is a valuable resource to the grid, and implies the ecopower could be a valuable demand response asset if configured to be able to receive grid requests. These data show that a fleet of variable output mCHP devices could provide grid support that is expected to become increasingly necessary, all while operating at a higher second law efficiency than most current residential heating systems.

Though the ecopower shows promise with regards to its technical performance, its capital cost is a large barrier to widespread adoption. The combination of high historic R&D costs and current low production volume has resulted in a capital cost that is approximately an order of magnitude larger than current gas furnace and air-source heat pumps. Techno-economic analyses have shown that this up-front cost is the primary driver in market penetration of mCHP devices [39]. As such, reductions in this metric must be achieved for the ecopower to be an economically viable grid-support generator.

3.1.3. System Emissions

Dilute post-catalyst emission measurements were recorded in triplicate at each of the load points. The composite measurements were calculated following a test cycle that was intended to mirror a 5-mode B-Cycle [40 CFR 1054 Appendix II(a)] steady-state test. However, the somewhat autonomous generator control system did not allow for the direct control of engine load, allowing only for engine speed to be controlled. The weighting factors for the composite emissions were

362 therefore adjusted to account for only engine speed (instead of load), and are shown in Table 4. The
363 emission measurements and relevant EPA standards [40] are given in Table 3. The measurements
364 show that all relevant emissions were below the standards by at least an order of magnitude.

Table 3. Composite brake emission measurements for the ecopower.

Composite Brake Emissions	[g/kWh]	Standard [g/kWh]
BSCO	1.76	610
$BSCO_2$	804.3	
BSTHC	6.97	
$BSNO_x$	0.70	
$BS(THC+NO_x)$	7.68	
$BSCH_4$	6.971	
BSNMHC	0.000	
$BS(NMHC+NO_x)$	0.706	8.0
BSN_2O	0.140	
BSFC	310.967	

Table 4. Mode weighting factors for composite emission calculations.

Test Cycle	Mode Weighting Factors				
	1	2	3	4	5
Torque [%] (Speed [RPM])	100 (3600)	75 (2700)	50 (1900)	25 (1500)	10 (1200)
Alt B Cycle	0.09	0.21	0.31	0.32	0.07

365 *3.2. Internal Combustion Engine Subsystem*

366 The ecopower's prime mover is a single cylinder, liquid cooled, natural gas fueled internal
367 combustion engine called the Marathon Engine. Briggs and Stratton, under direction from the Gas
368 Technology Institute, initially designed this engine for use in an ICE-driven heat pump. The engine's
369 specifications are given in Table 5.

Table 5. Tables of the relevant ecopower specifications.

Engine Specifications	
Engine Name	Marathon Engine
Number of Cylinders	1
Engine Speed	1200-3600 [RPM]
Displacement	272 [cm^3]
Bore	7.3 [cm]
Stroke	6.5 [cm]
Fuel Consumption (Natural Gas)	22.2-68.6 [MJ/h]
Alternator Specifications	
Rated Maximum Continuous Power	7,000 W
Rated Voltage	240 V
Rated Maximum Continuous Current	30 A
Genset Specifications	
Length	1.37 [m]
Width	0.76 [m]
Height	1.1 [m]
Endurance	40,000 [h]

The ICE is responsible for converting the chemical energy stored within the fuel into mechanical shaft work. The remaining energy leaves as either chemical or thermal energy in the exhaust, or through heat transfer that is either recovered or unrecovered, Figure 7.

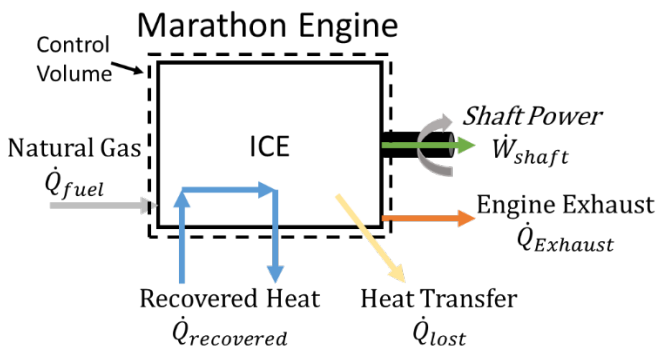

Figure 7. ICE system diagram including energy flows across control volume.

As was discussed in Section 2.4, it was not possible to directly measure the shaft power output by the engine due to the ecopower's sophisticated control system. Therefore, the output shaft power was calculated using the electrical power produced by the ecopower, and the measured generator efficiency (discussed in the forthcoming section). The exhaust temperature was measured using a custom fabricated exhaust manifold with an integrated thermocouple which allowed for calculation of the thermal energy present in the exhaust. Direct engine emission measurements were not taken at

the engine exhaust due to resource constraints. As such, the engine exhaust (pre-catalyst) was assumed to have the same composition as the system-level emissions (post-catalyst). The recovered heat was calculated by measuring the coolant temperature before and after the engine coolant passages, as well as the flowrate through the coolant loop. This accounted for the energy flows crossing the control surfaces.

Several losses that occurred within the control volume are of interest to engineers that were unaccounted for in these energy flows crossing control surfaces; namely: frictional and pumping losses. To measure these losses, in-cylinder pressure measurements were recorded at greater than 0.2 crank angle degree increments at each of the engine operating speeds. Using the known engine geometry, the in-cylinder pressure measurements were used to calculate the GIMEP, the PIMEP, and the NIMEP produced by the engine, Figure 8. The GIMEP is the mean effective pressure during the compression and power stroke of the engine, and is a measure of the power produced during combustion. The PIMEP is the mean effective pressure during the time that gas was being pumped into and out of the cylinder (when the intake or exhaust valves are open), and is a direct measure of the power consumed to intake fresh air-fuel mixture and exhaust the combustion products. The NIMEP is the GIMEP less the PIMEP, and is a measure of the net power produced over the entire 4-stroke engine cycle. This is a direct measure of the useful indicated power the engine can produce after pumping losses are accounted for.

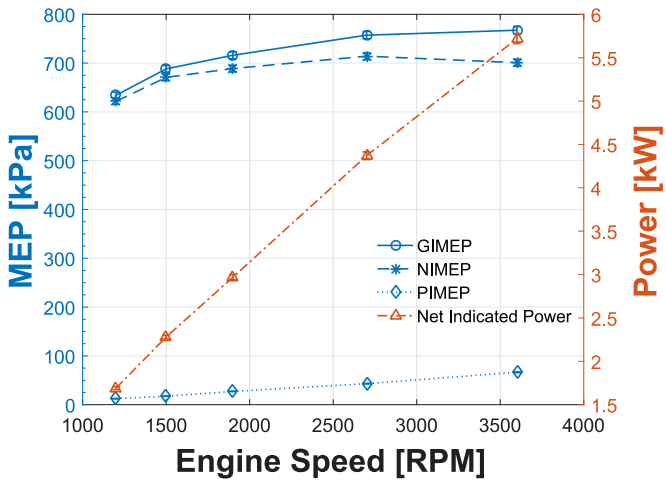

Figure 8. Mean effective pressure and indicated pressure as a function of engine speed.

The net indicated power is plotted in Figure 8, and is nearly a linear function of engine speed. The pumping losses increased with engine speed, but were less than approximately 10% of the gross indicated power over all engine speeds. The frictional loss within the engine was calculated by

subtracting the connecting rod brake shaft power (calculated from the generator efficiency and generator electrical output as described in the forthcoming section) from the measured net indicated power. With the losses internal to the control volume (friction and pumping) calculated, and the streams crossing the control surfaces measured, a component-level energy and exergy balance was conducted on the Marathon Engine, shown in Figure 9 through Figure 12.

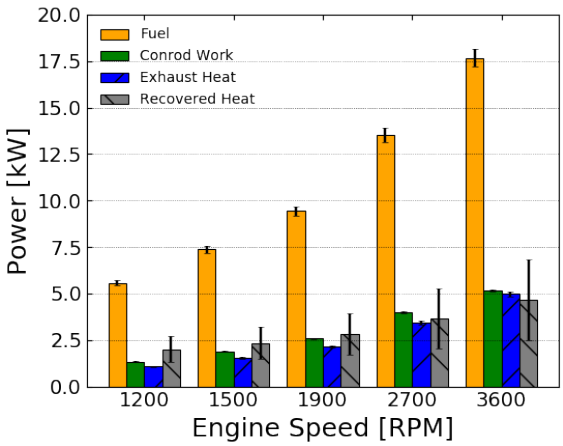

Figure 9. Major components of the first law energy balance on the engine.

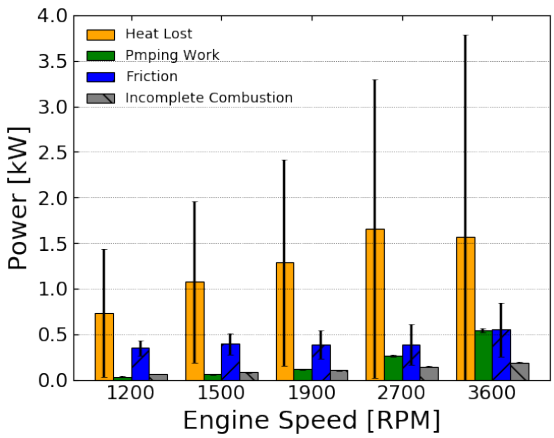

Figure 10. Minor components of the first law energy balance on the engine.

Figure 9 and Figure 10 show the major and minor components of the energy balance (note the difference in ordinate scales), respectively. The major components (connecting rod brake shaft work, heat in the exhaust, and the recovered heat) were relatively balanced, with all power flows increasing with engine speed. The minor components were less structured. Lost heat (heat transferred from the engine but not into the coolant) was the largest minor component at each engine speed by a wide margin. Frictional loss was somewhat constant until an increase was seen at the higher engine speeds. It should be noted that this measure of friction only includes friction between the piston rings and the cylinder, and the connecting rod bearing. It does not include main bearing friction due to the apparatus used to measure the generator efficiency (Section 3.3). Pumping work showed a positive power fit to the engine speed, and was roughly equal in magnitude to friction at 3600 RPM.

At rated speed, the shaft power produced, heat present in the exhaust, and heat recovered into the engine coolant were all comparative in magnitude. At rated speed, the engine operated at a connecting rod brake efficiency of 29.3±0.9 %, with 26.4±12.3% of the input energy recovered into the coolant, and 28.2±0.1% present as thermal energy in the exhaust. This equates to an engine utilization factor of 55.7±12.4%, highlighting the necessity of the exhaust gas, oil, and generator heat

exchangers.

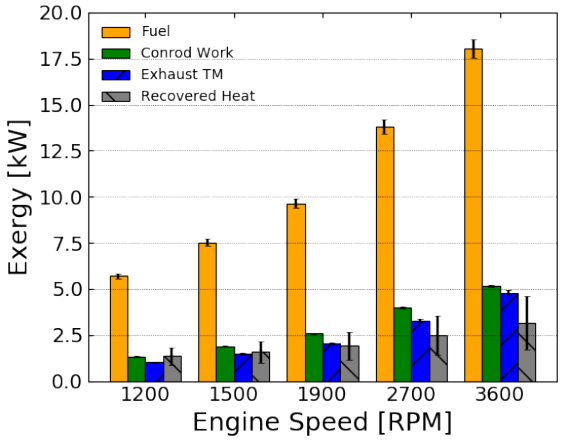

Figure 11. Major components of the second law exergy balance on the engine.

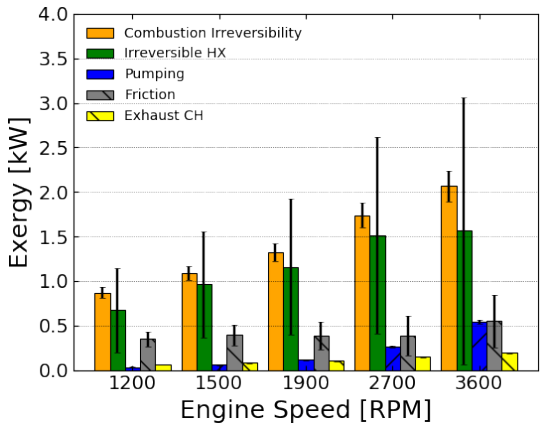

Figure 12. Minor components of the second law exergy balance on the engine.

The exergy balance on the Marathon Engine is presented in Figure 11 and Figure 12. In descending order, the largest contributions to the exergy balance at rated power were the connecting rod work produced, the thermomechanical exergy in the exhaust, heat recovered in the coolant, combustion irreversibility, irreversible (including uncaptured) heat transfer, irreversible pumping work, friction irreversibility, and finally the chemical exergy present in the exhaust (note that this is calculated from post-catalyst emission measurements).

The second law efficiency of the connecting rod work stream was highest at the higher engine speeds of 2700 and 3600 RMP, reaching a peak of 28.7 ± 0.9% at both of these speeds. This is a rather impressive result for an engine in the 5 kW range. For example, Primus et al. measured a 224 kW six-cylinder, turbocharged and aftercooled, diesel engine operating at 2100 RPM to have shaft-work based second law efficiency of 39.21% [41], [42]. Therefore, the ecopower sees an approximately 10% second law efficiency reduction from an engine that has cylinders with roughly six times the displacement. The ecopower's second law efficiency also compares favorably to the other mCHP and residential backup generators that were tested. The Honda ECOWILL (1 kWe) and Generac 8 kW Guardian were measured to have second law efficiencies of 27.2% [32] and 24.4% [5], respectively. The improvement over the ECOWILL is believed to be due to a more favorable cylinder volume to surface area ratio which results in lower heat transfer. Higher quality components and a higher level of engine optimization are believed to be responsible for the ecopower's increased performance over the Guardian.

The ecopower's exergy efficiency mirrored the energy efficiency results by increasing at

higher engine speeds. The exergy accounting revealed that the largest measured irreversibility was the combustion irreversibility, closely followed by irreversible heat transfer (including heat that was not captured into the coolant). At low engine speeds the friction irreversibility was somewhat significant while the pumping irreversibility was not. However, as engine speed increased, neither the pumping nor friction irreversibility proved to be significant.

3.3. Electric Generator and Power Electronics Subsystem

After the engine converts the stored chemical energy to shaft work, the electric generator converts the shaft work into high frequency 3-phase electrical work. The high-frequency three phase electricity is then converted into 120 Hz, 240V, single phase electricity by the power electronics. This electricity pathway is shown in Figure 13.

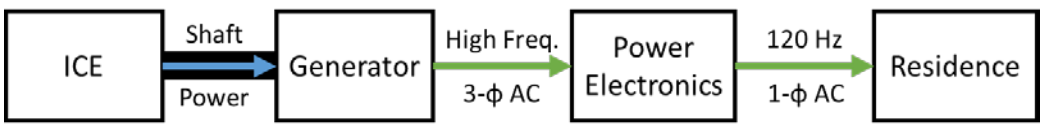

Figure 13. Energy conversions from ICE to the residence.

In this testing campaign it was infeasible to measure the power electronics efficiency due to available sensors, space constraints, and DAQ channels. Thus, a power electronic efficiency of 91 % was assumed based on manufacturer specification sheets. To determine the losses associated with the generator, the electric generator underwent performance testing via dynamometer as outlined in Section 2.4. The generator was run at 4 different speeds: 1200, 1700, 2500, and 3500 RPM. The electronic load was swept over a series of loads at each of the speed set points, producing a curve for each of the operating speeds. Then, the input power measured at the torque transducer and the output electrical power was used to calculate the electrical generator efficiency, which is presented in Figure 14.

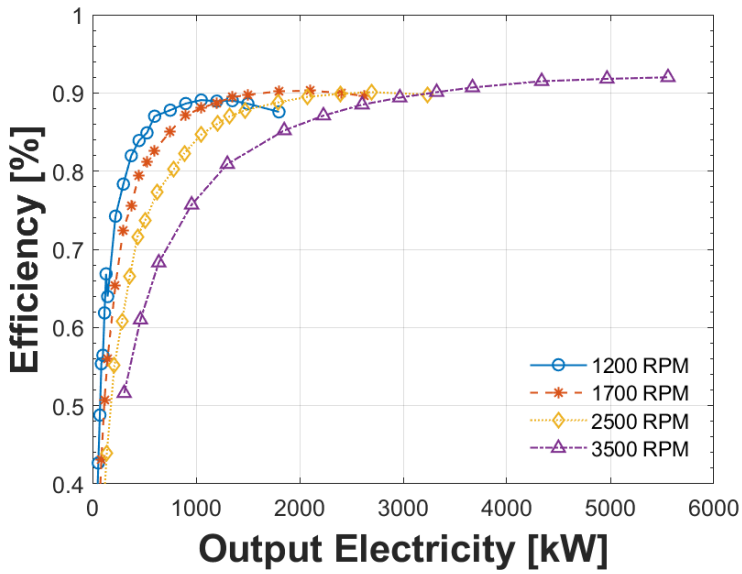

Figure 14. Electric generator efficiency as a function of rotational speed and power output.

These data show that the generator operates at approximately 90 % efficiency over the entire electrical output range of 1 – 4.5 kWe. For example, at an engine/generator speed of 1200 RPM the electric generator generates about 1.2 kWe (measured before the power electronics). Following the line with circle symbols, the generator would operate at an efficiency of approximately 88%. At an engine/generator speed of 3600 RPM the generator was measured to produce 4.75 kWe. Following the line with triangle symbols the generator can be seen to operate at approximately 92 % efficiency. At intermediate speeds the generator maintains an efficiency of about 90 %.

Using the electrical power measured after the power electronics, the assumed power electronic efficiency and the measured generator efficiency, the connecting rod brake shaft power was calculated. Since the main bearing friction was included in the generator efficiency, the brake vales reported are calculated at the connecting rod instead of the crankshaft.

3.4. Heat Recovery Loop

Like other mCHP devices, the ecopower is designed to capture heat from nearly every available source within the system. The ecopower's stock coolant loop collects heat in the following order: electric generator, oil cooler, exhaust gas heat exchanger, and then the engine. However, in an attempt to quantify the performance trade-offs that rerouting the heat recovery loop could have, the recovery order was re-configured as such: electric generator, oil cooler, engine, and then the exhaust gas heat exchanger. This was done for comparison purposes with other published results in the literature to determine if an increase in heat recovery or electrical efficiency could be achieved. As is annotated in Figure 1, thermocouples were installed on either side of each heat recovery device to

measure each device's contribution to the total heat recovery. These data are presented in Figure 15.

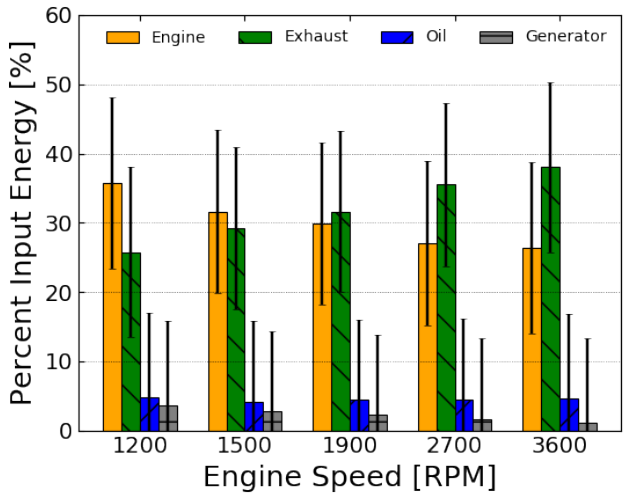

Figure 15. Heat recovery of each device in the ecopower's heat recovery loop.

For all engine speeds, the ecopower recovered a majority of its heat from the exhaust gas and the internal combustion engine heat exchangers. In comparison to the engine and exhaust gas exchangers, the oil cooler and generator provided relatively low amounts of heat. However, combined they recovered approximately 7 % of the input power, thereby increasing the ecopower's utilization factor by the same amount.

At low engine speeds the majority of the heat was recovered from the internal combustion engine, followed by heat recovery from the exhaust gasses. However, as the engine speed increased, this trend reversed. At the rated engine speed (3600 RPM) the majority of the heat was recovered from the exhaust gas. It is believe this was due to the reduction in heat transfer to the engine cylinder walls, as there was a decrease in residence time of the hot combustion products in the engine cylinder at higher engine speeds. This reduction in relative heat transfer was further elucidated by the increase in engine exhaust temperature. As engine speed increased the engine exhaust temperature increased from approximately 480 °C at 1200 RPM to 680 °C at 3600 RPM, indicating that a larger portion of energy was remaining in the exhaust as opposed to transferring into the cylinder walls.

4. Conclusion

A Marathon Engine Systems ecopower was selected to undergo thermodynamic performance testing due to its high utilization factor and its uncommon ability to modulate its thermal and electrical output. First and second law system-level analysis were conducted to assess the ecopower's utilization factor, as well as its potential to provide grid-support ("ancillary") services in a future with increased

penetration of variable electricity generators. Component-level (ICE and electric generator) analysis were conducted to identify inefficiencies and irreversibilities within the subsystems that must be improved to increase the performance of the ecopower in specific, and mCHP generators in general. Key findings from this study were:

- The ecopower operated at an electrical efficiency and utilization factor of 24.4±0.9 % and 94.5±12.6 %, respectively.
- The ecopower's second law electrical and total exergy efficiency was 24.3±0.8 % and 33.7±1.9 % respectively.
- The ecopower's ICE operated at a connecting rod brake first and second law efficiency of 29.3±0.9 %, and 28.7±0.9 %, respectively.
- The ecopower's electric generator maintained an efficiency (when including main bearing friction) above 88% over all operating speeds, including 92 % at rated speed.

The system-level measurements show the ecopower can operate at a higher second law efficiency than most other residential heating technologies (i.e., furnaces, engine-driven and electric air-source heat pumps, boilers), even when operating at part load. This indicates that variable-output, dispatchable, mCHP generators, such as the ecopower, can efficiently provide grid-support services by operating at part-load and then ramping output up or down to respond to gird requests. The largest system-level energy losses were uncaptured heat transfer from the device, followed by thermal and chemical energy present in the exhaust. However, the ecopower was effective in converting and recovering energy present in the exhaust, leaving only 4% of the input energy in the exhaust at rated speed. Though the recovered heat provides a direct energy boost from the first law perspective, it only marginally improves the second law efficiency. To increase the ecopower's second law efficiency, improvements in generating and retaining mechanical and electrical work need to be prioritized over recovering heat. In particular, efficiency improvements to the ICE need to be prioritized as they will have the largest impact on system-level exergy efficiency (e.g., a 2% increase in ICE efficiency yields a 1.7% increase in system-level efficiency while a 2% increase in generator or power electronics yields a 0.5% system-level efficiency increase). Some advanced technologies that have the potential to improve engine efficiency are advanced combustion technologies such as homogeneous charge compression ignition (to reduce heat transfer), alternative thermodynamic cycles such as the Atkinson cycle (to reduce pumping losses), and in-cylinder energy retention techniques such as thermal insulation coatings.

The device-level ICE analysis revealed that the largest energy loss was unrecovered heat transfer, while the largest source or exergy destruction was combustion irreversibility. There was a clear division between major and minor energy flows from the engine. The major flows comprised: shaft work, exhaust thermal energy, and recovered heat. The minor flows comprised: unrecovered

549 heat, pumping wok, friction losses, and incomplete combustion.

550 Acknowledgements

551 The information, data, or work presented herein was funded in part by the Advanced Research
552 Projects Agency-Energy (ARPA-E), U.S. Department of Energy, under Award Number DE-
553 AR0000485.

554 The authors would like to thank Marathon Engine Systems for graciously donating an
555 ecopower for performance testing. Further, the authors would like to thank Marathon Engine Systems
556 for fabricating custom components that enabled difficult sensor placement, and for their assistance in
557 installing the ecopower at the testing facility to replicate field installation.

558 References

559 [1] G. A. Richards, “New Combustion Technologies – Promise and Progress.” 2017 Princeton-Combustion Institute Summer School
560 on Combustion, Princeton, NJ, 2017.
561 [2] GE, “BREAKING THE POWER PLANT EFFICIENCY RECORD...AGAIN!,” *ge.com/power*, 2018. [Online]. Available:
562 https://www.ge.com/power/about/insights/articles/2018/03/nishi-nagoya-efficiency-record. [Accessed: 07-Jan-2018].
563 [3] The World Bank, “Electric power transmission and distribution losses (% of output),” *data.worldbank.org*, 2018. [Online].
564 Available: https://data.worldbank.org/indicator/EG.ELC.LOSS.ZS. [Accessed: 07-Jan-2018].
565 [4] U.S. Energy Information Administration (EIA), “State Electricity Profiles,” 2018. [Online]. Available:
566 https://www.eia.gov/electricity/state/. [Accessed: 07-Jan-2018].
567 [5] Z. Taie, W. Beckwith, and C. Hagen, “First and second law thermodynamic analysis of a natural gas fueled residential standby
568 generator,” in *2016 Spring Technical Meeting of the Western States Section of the Combustion Institute, WSSCI 2016*, 2016.
569 [6] U. Arndt, I. Beausoleil-Morrison, M. Davis, W. D’haeseleer, V. Dorer, E. Entchev, A. Ferguson, J. Gusdorf, N. Kelly, M.
570 Manning, L. Peeters, M. Sasso, D. Schreiber, S. Sibilio, K. Siemens, and M. Swinton, *Experimental Investigation of Residential*
571 *Cogeneration Devices and Calibration of Annex 42 Models*. 2007.
572 [7] Advanced Research Project Agency - Energy, “GENSETS,” 2015. [Online]. Available: https://arpa-e.energy.gov/?q=arpa-e-
573 programs/gensets. [Accessed: 07-Jan-2018].
574 [8] Z. Taie and C. Hagen, “Final Scientific/Technical Report - Home Generator Benchmarking Program,” Bend, Oregon, 2016.
575 [9] S. Murugan and B. Horak, “A review of micro combined heat and power systems for residential applications,” *Renew. Sustain.*
576 *Energy Rev.*, vol. 64, pp. 144–162, 2016.
577 [10] A. A. Aliabadi, M. J. Thomson, and J. S. Wallace, “Efficiency analysis of natural gas residential micro-cogeneration systems,”
578 *Energy and Fuels*, vol. 24, no. 3, pp. 1704–1710, 2010.
579 [11] M. Ebrahimi and A. Keshavarz, “Prime mover selection for a residential micro-CCHP by using two multi-criteria decision-
580 making methods,” *Energy Build.*, vol. 55, pp. 322–331, 2012.
581 [12] A. D. Hawkes and M. A. Leach, “Cost-effective operating strategy for residential micro-combined heat and power,” *Energy*, vol.
582 32, no. 5, pp. 711–723, 2007.
583 [13] H. Ren and W. Gao, “Economic and environmental evaluation of micro CHP systems with different operating modes for
584 residential buildings in Japan,” *Energy Build.*, vol. 42, no. 6, pp. 853–861, 2010.
585 [14] A. Rosato, S. Sibilio, and G. Ciampi, “Energy, environmental and economic dynamic performance assessment of different micro-
586 cogeneration systems in a residential application,” *Appl. Therm. Eng.*, vol. 59, no. 1–2, pp. 599–617, 2013.

[15] S. Sanaye, M. A. Meybodi, and S. Shokrollahi, “Selecting the prime movers and nominal powers in combined heat and power systems,” *Appl. Therm. Eng.*, vol. 28, no. 10, pp. 1177–1188, 2008.

[16] J. Sarkar and S. Bhattacharyya, “Operating characteristics of transcritical CO2 heat pump for simultaneous water cooling and heating,” *Arch. Thermodyn.*, vol. 33, no. 4, pp. 23–40, 2012.

[17] O. A. Shaneb, G. Coates, and P. C. Taylor, “Sizing of residential uCHP systems,” *Energy Build.*, vol. 43, no. 8, pp. 1991–2001, 2011.

[18] H. I. Onovwiona and V. I. Ugursal, “Residential cogeneration systems: Review of the current technology,” *Renew. Sustain. Energy Rev.*, vol. 10, no. 5, pp. 389–431, 2006.

[19] S. R. Asaee, V. I. Ugursal, and I. Beausoleil-Morrison, “An investigation of the techno-economic impact of internal combustion engine based cogeneration systems on the energy requirements and greenhouse gas emissions of the Canadian housing stock,” *Appl. Therm. Eng.*, vol. 87, pp. 505–518, 2015.

[20] S. R. Asaee, V. I. Ugursal, and I. Beausoleil-Morrison, “Techno-economic evaluation of internal combustion engine based cogeneration system retrofits in Canadian houses - A preliminary study,” *Appl. Energy*, vol. 140, pp. 171–183, 2015.

[21] E. S. Barbieri, F. Melino, and M. Morini, “Influence of the thermal energy storage on the profitability of micro-CHP systems for residential building applications,” *Appl. Energy*, vol. 97, pp. 714–722, 2012.

[22] E. S. Barbieri, P. R. Spina, and M. Venturini, “Analysis of innovative micro-CHP systems to meet household energy demands,” *Appl. Energy*, vol. 97, pp. 723–733, 2012.

[23] M. Bianchi, A. De Pascale, and F. Melino, “Performance analysis of an integrated CHP system with thermal and Electric Energy Storage for residential application,” *Appl. Energy*, vol. 112, pp. 928–938, 2013.

[24] M. Bianchi, A. De Pascale, and P. R. Spina, “Guidelines for residential micro-CHP systems design,” *Appl. Energy*, vol. 97, pp. 673–685, 2012.

[25] M. De Paepe, P. D’Herdt, and D. Mertens, “Micro-CHP systems for residential applications,” *Energy Convers. Manag.*, vol. 47, no. 18–19, pp. 3435–3446, 2006.

[26] D. Beyer and N. Kelly, “Modelling the behaviour of domestic micro-cogeneration under different operating regimes and with variable thermal buffering.,” in *1st International Conference on Micro-Cogeneration Technologies and Applications*, 2009.

[27] G. Chicco and P. Mancarella, “A unified model for energy and environmental performance assessment of natural gas-fueled poly-generation systems,” *Energy Convers. Manag.*, vol. 49, no. 8, pp. 2069–2077, 2008.

[28] V. Dorer and A. Weber, “Energy and CO2 emissions performance assessment of residential micro-cogeneration systems with dynamic whole-building simulation programs,” *Energy Convers. Manag.*, vol. 50, no. 3, pp. 648–657, 2009.

[29] V. Dorer and A. Weber, “Energy and carbon emission footprint of micro-CHP systems in residential buildings of different energy demand levels BT - Modelling Cogeneration Systems,” *J. Build. Perform. Simul.*, vol. 2, no. 1, pp. 31–46, 2009.

[30] A. Rosato, S. Sibilio, and G. Ciampi, “Dynamic performance assessment of a building-integrated cogeneration system for an Italian residential application,” *Energy Build.*, vol. 64, pp. 343–358, 2013.

[31] H. I. Onovwiona, V. Ismet Ugursal, and A. S. Fung, “Modeling of internal combustion engine based cogeneration systems for residential applications,” *Appl. Therm. Eng.*, vol. 27, no. 5–6, pp. 848–861, 2007.

[32] Z. Taie, B. West, J. Szybist, D. Edwards, J. Thomas, S. Huff, G. Vishwanathan, and C. Hagen, “Detailed thermodynamic investigation of an ICE-driven, natural gas-fueled, 1 kWe micro-CHP generator,” *Energy Convers. Manag.*, vol. 166, no. April, pp. 663–673, 2018.

[33] Power Systems Research, “OSU PartsLink Data File Portable Gen Sets,” St. Paul, MN, 2014.

[34] M. A. Rosen and C. A. Bulucea, “Using exergy to understand and improve the efficiency of electrical power technologies,” *Entropy*, vol. 11, no. 4, pp. 820–835, 2009.

[35] L. Yang, R. Zmeureanu, and H. Rivard, “Comparison of environmental impacts of two residential heating systems,” *Build. Environ.*, vol. 43, no. 6, pp. 1072–1081, 2008.

[36] S. A. Klein and G. Nellis, *Thermodynamics*. Cambridge University Press, 2012.

[37] E. Nieuwlaar and D. Dijk, “Exergy evaluation of space-heating options,” *Energy*, vol. 18, no. 7, pp. 779–790, 1993.

[38] Y. Xie, C. Liu, and Z. Yu, “ENERGY GRADE BALANCE OF GAS ENGINE-DRIVEN HEAT PUMP,” *Proc. ASME Int. Sol.*

633 *Energy Conf.*, pp. 1–4, 2006.
634 [39] G. Vishwanathan, J. P. Sculley, A. Fischer, and J.-C. Zhao, “Techno-economic analysis of high-efficiency natural-gas generators
635 for residential combined heat and power,” *Appl. Energy*, vol. 226, no. April, pp. 1064–1075, 2018.
636 [40] US EPA, *Nonroad Spark-Ignition Engines 19 Kilowatts and Below: Exhaust Emission Standards*, no. March. 2016, pp. 1–2.
637 [41] R. Primus and P. F. Flynn, “The assessment of losses in diesel engines using second law analysis,” in *Proceedings of the AES*,
638 1986, pp. 61–68.
639 [42] R. Primus and P. Flynn, “Diagnosing the Real Performance Impact of Diesel Engine Design Parameter Variation (A Primer in
640 the Use of Second Law Analysis),” in *Proceedings of International Symposium on Diagnostics and Modeling Combustion in*
641 *Reciprocating Engines*, 1985, pp. 529–538.
642